1556

SEISMIC RESPONSE OF NON LINEAR STRUCTURES USING THE CONCEPT OF VARIABLE DAMPING RESPONSE SPECTRUM

Tommaso ALBANESI[1], Camillo NUTI[2] And Ivo VANZI[3]

SUMMARY

An improvement of the iterative ATC procedure, herein referred to as Variable Damping Response Spectrum, VDRS, to evaluate the seismic response of non linear structures in terms of maximum displacement and acceleration, given the initial elastic period and yielding acceleration has been presented by the authors in previous works [Albanesi et al., 1999a,b]. The VDRS improvement consists in a simplification of the original ATC iterative procedure and furnishes the same results in a faster way. This paper, while referring to the previous ones for the methodological part of VDRS, presents an extended set of numerical tests is presented and it is shown that simpler traditional methods, such as equal energy and equal displacement assumptions, look as accurate. However the ATC procedure permits to take into account complex structural behavior, more representative of real structural response.

INTRODUCTION

Seismic evaluation of existing reinforced concrete structure requires estimation of the structural performances in terms of acceleration and displacement. In [ATC, 1996] an iterative procedure to obtain these values is proposed, departing from the structural push over curve, i.e. a curve where base shear versus roof displacement is given. The procedure is conceptually simple but time consuming and therefore the authors decided to find possible simplifications. In previous papers [Albanesi et al., 1999a,b] this simplification, which yields the same results as the ATC procedure, was presented and tested again the results of numerical simulations. In this paper an extended set of numerical tests is presented and it is shown that simpler traditional methods, such as equal energy and equal displacement assumptions, look as accurate. However the ATC procedure permits to take into account complex structural behavior, more representative of real structural response. Since it is well known that the validity of such simplified procedure, where the nonlinear behavior is linearized to obtain structural response, must be proved. Here the check is done comparing the results of the ATC procedure, which coincides with those of the VDRS method, with the traditional equal energy equal displacement assumption, and with numerical step by step simulation. Results show that, though the ATC procedure seems more rigorous, at least for the elasto-plastic case, simpler rules are as precise if not more. However while the simple equal energy, equal displacement assumption cannot take into account more complicate and more adherent to real behavior models the ATC method can take into account them, thus remaining valid as well. In what follows, only the results of the numerical tests will be presented while referring to [Albanesi et al., 1999a,b] for the VDRS method.

COMPARISON OF VDRS WITH RESULTS FROM ARTIFICIAL AND NATURAL ACCELEROGRAMS

To assess the accuracy of the VDRS procedure the results obtained with the VDRS have been compared to those obtained by numerical simulation with synthetic and natural accelerograms and with simpler approaches, namely equal energy (EE) and equal displacement (ED) assumptions. Two structural model are considered: the elasto-yielding model and the Takeda one with degrading stiffness:

[1] *Dipartimento di Sciemze, Storia dell'Architettura e Restauro, Università G. D'Annunzio di Chieti, Viale Pindaro*
[2] *Dipartimento di Sciemze, Storia dell'Architettura e Restauro, Università G. D'Annunzio di Chieti, E-mail: nuti@unich.it*
[3] *Dipartimento di Sciemze, Storia dell'Architettura e Restauro, Università G. D'Annunzio di Chieti, Viale Pindaro*

$$k_s = k_e \sqrt{\frac{d_y}{d}} \tag{1}$$

k_e being the elastic stiffness of the structure and d_y the spectral yield displacement.

It is recalled that, indicating the period of maximum value of the (linear) acceleration response spectrum with T_{peak}, EE is applicable for $0<T_e<T_{peak}$ whereas ED for $T_e>T_{peak}$ [Gulkan, 1977]. From this point on, EE and ED assumptions, in the respective field of applicability, will be referred to as EE-ED model.

Results are somehow dependent on the accelerograms considered, whether artificial or natural and, in the latter case, on the type of soil on which they are recorded. However here mean values over the entire set of parameters are given.

The complete test program has therefore comprehended the following:

- $VDRS_{NL}$ and $VDRS_{12}$ vs EE-ED model and PP's computed using artificial accelerograms;

- $VDRS_{NL}$ and $VDRS_{12}$ vs EE-ED model and PP's computed using natural accelerograms;

for sdof elasto-yielding oscillators with full hysteretic cycles and for sdof systems with degrading Takeda model, with α ranging from 0.1 to 1.0, step 0.1 (α being the ratio between the spectral yield acceleration a_y and the acceleration $a_D(T_e, 5\%, a_g)$ which would occur if the structure remained perfectly elastic for a specified earthquake with peak ground acceleratoin a_g,), elastic period T_e=(0.2; 0.4; 0.6; 1.0; 1.5) sec and ratio between the post-elastic and the elastic stiffness p=5% and 25%.

Testing scheme for artificial accelerograms

From EC8 response spectrum, soil type B, eighteen spectrum compatible time histories have been generated using the program SIMQKE, nine samples having a duration of 20 s, nine samples of 40 s.

For each elastic period, the accelerograms have been used as input motion for the bilinear and Takeda structures having the specified T_e, p and α. Coefficient of variation of results, not shown here, have usual values, about 30%, decreasing for the cases which tend towards the linear behavior i.e. p=25% and/or α=1.0.

The difference in the results of the 20 and 40 sec. samples has proved negligible. Therefore, only the results of the 20 sec. samples were retained for comparison.

For each model ($VDRS_{NL}$, $VDRS_{12}$, EE-ED), results are presented in terms of difference Δ between the displacements of the model and the target (the mean value of the numerical simulations), adimensionalized to the target result and plotted in a (α, Δ) diagram for each p and T_e:

$$\Delta(model, T_e, p, \alpha) = \frac{d_{C\max}(model, T_e, p, \alpha) - \bar{d}_{C\max}(a.a., T_e, p, \alpha)}{\bar{d}_{C\max}(a.a., T_e, p, \alpha)} \tag{2}$$

in which a.a.=artificial accelerograms and the overscore sign indicates the mean on the artificial accelerograms.

Testing scheme for natural accelerograms

The natural accelerograms chosen for the simulations are a subset of those listed in [Miranda, 1993] and include 6 samples recorded on rock, 8 on alluvium and 2 on soft soil. These samples were recorded in the events of Loma Prieta 17.10.1989, 7.1 (M_S) and Whitter-Narrows 1.10.1989, 6.1 (M_L), indicated respectively with the letters "l" and "w" in the table.

Table 1. Natural accelerograms

site type	earth-quake	station name	geology	epicentral dist. (km)	component		pga (g)
rock	l	corralitos	landslide deposits	7	90	360	0.62
rock	l	santa cruz	limestone	16	90	360	0.41
rock	l	san francisco pacific heights	franciscan sandstone	97	270	360	0.05
rock	l	san francisco presidio	serpentine	98	90	360	0.20
rock	l	san francisco rincon hill	franciscan sandstone	95	90	360	0.09
rock	l	yerba buena island	franciscan sandstone	95	90	360	0.06
alluvium	w	alhambra	alluvium	7	180	270	0.40
alluvium	w	altadena	alluvium	13	90	360	0.31
alluvium	w	downey	deep alluvium	17	180	270	0.20
alluvium	w	inglewood	terrace deposits	25	90	180	0.27
alluvium	w	los angeles baldwin hills	alluvium over shale	27	0	90	0.17
alluvium	w	tarzana	alluvium	44	0	90	0.63
alluvium	l	capitola	alluvium	9	90	360	0.39
alluvium	l	hollister	alluvium	48	90	360	0.17
soft	l	foster city	bad mud	79	90	360	0.28
soft	l	san francisco intern. airport	bad mud	63	90	360	0.33

The samples are representative of medium to intense events (M 6.1-7.1) recorded from very near the epicentral location to moderate distances (7-98 Km) and should thus be sufficiently representative of the randomness in the earthquake frequency content. Each of these events has been first scaled to 1 m/s^2 p.g.a. and then its linear response spectrum computed. With it, the $VDRS_{NL}$, $VDRS_{12}$ and EE-ED models have been applied for the tested T_e, p and α. The event itself has then been used as the input motion for an elasto - yielding oscillator with full hysteretic cycles and for a Takeda degrading sdof, having the prescribed properties (T_e, α, p) and the difference δ in the maximum displacement has been computed as:

$$\delta(model, event, T_e, p, \alpha) = \frac{d_{C\max}(model, n.a., T_e, p, \alpha) - d_{C\max}(num.sim., n.a., T_e, p, \alpha)}{d_{C\max}(num.sim.; n.a.,, T_e, p, \alpha)} \qquad (3)$$

where n.a. indicates natural accelerograms. δs have been first examined by soil type, distinguishing results pertaining to rock, alluvium and soft soils.

Since no interesting piece of information appeared from the grouping in these categories, for the sake of conciseness results have been put together, irrespective of the soil type, so as to compute, for each oscillator (T_e, α, p) the value of the error Δ:

$$\Delta(model, T_e, p, \alpha) = \bar{\delta}\left(model, n.a., T_e, p, \alpha\right) \qquad (4)$$

where the overscore sign indicates the averaging operation over earthquakes.

Results

The error Δ as a function of α for α=0.1, 0.2, ..., 1.0 and fixed values of p and T_e for both artificial and natural accelerograms is shown in figures 1 - 40 organized as follows: the first group of four rows (Fig. 1-20) refers to the elasto-yielding model, the second (Fig. 21-40) refers to the Takeda degrading model; each column is relative to one value for T_e (from left to right, T_e=0.2; 0.4; 0.6; 1.0; 1.5 sec); for each group the first two rows refer to the natural accelerograms (respectively for p=5% e 25%) and the second to the artificial accelerograms (respectively for p=5% e 25%). Results of the EE-ED model (EE for T_e=0.2, *ED* for T_e≥0.6s, both for T_e=0.4s)) are shown with continuous lines with circle symbols; those of $VDRS_{NL}$ and $VDRS_{12}$ are both indicated with continuous lines with square symbols. They are coincident for high α values (in the range 0.7-1.0) and distinct for lower α values, with $VDRS_{12}$ being always above $VDRS_{NL}$.

elasto-yielding model

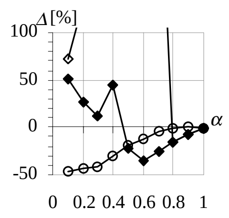

Figure 1. Δ
n.a. p=5% T_e=0.2

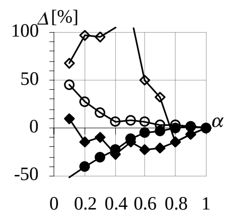

Figure 2. Δ
n.a. p=5% T_e=0.4

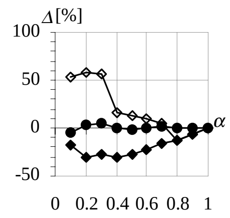

Figure 3. Δ
n.a. p=5% T_e=0.6

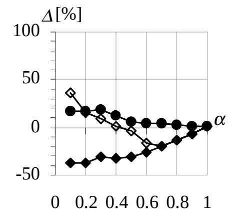

Figure 4. Δ
n.a. p=5% T_e=1.0

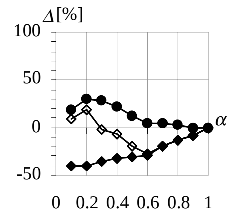

Figure 5. Δ
n.a. p=5% T_e=1.5

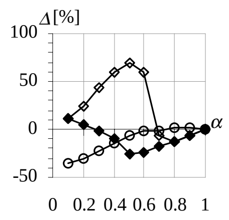

Figure 6. Δ
n.a. p=25% T_e=0.2

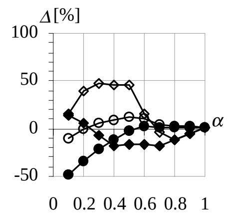

Figure 7. Δ
n.a. p=25% T_e=0.4

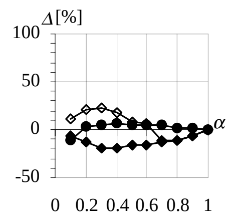

Figure 8. Δ
n.a. p=25% T_e=0.6

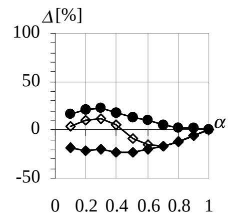

Figure 9. Δ
n.a. p=25% T_e=1.0

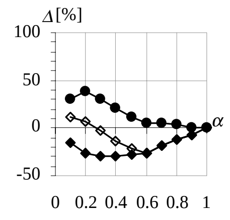

Figure 10. Δ
n.a. p=25% T_e=1.5

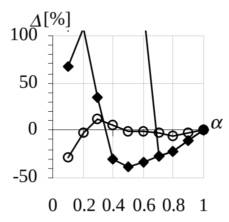

Figure 11. Δ
a.a. p=5% T_e=0.2

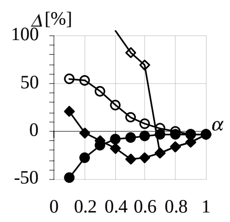

Figure 12. Δ
a.a. p=5% T_e=0.4

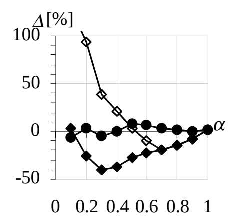

Figure 13. Δ
a.a. p=5% T_e=0.6

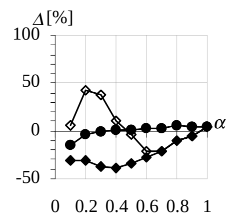

Figure 14. Δ
a.a. p=5% T_e=1.0

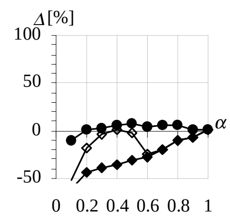

Figure 15. Δ
a.a. p=5% T_e=1.5

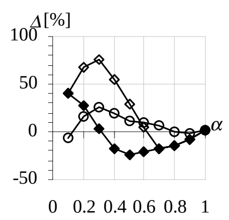

Figure 16. Δ
a.a. p=25% T_e=0.2

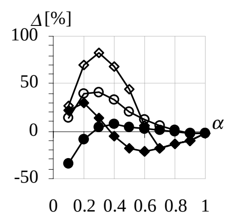

Figure 17. Δ
a.a. p=25% T_e=0.4

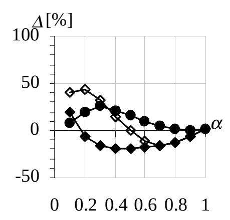

Figure 18. Δ
a.a. p=25% T_e=0.6

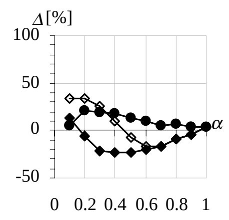

Figure 19. Δ
a.a. p=25% T_e=1.0

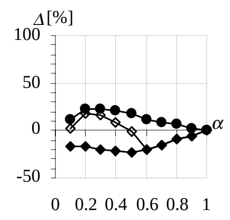

Figure 20. Δ
a.a. p=25% T_e=1.5

$VDRS_{NL}$ — $VDRS_{12}$ — EE — ED

Takeda degrading model

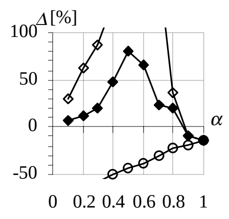

Figure 21. Δ
n.a. p=5% T_e=0.2

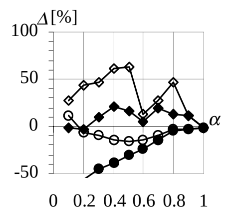

Figure 22. Δ
n.a. p=5% T_e=0.4

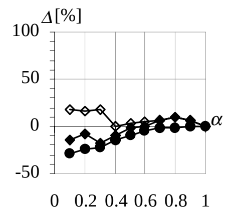

Figure 23. Δ
n.a. p=5% T_e=0.6

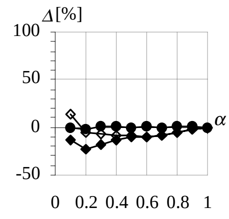

Figure 24. Δ
n.a. p=5% T_e=1.0

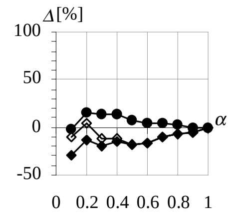

Figure 25. Δ
n.a. p=5% T_e=1.5

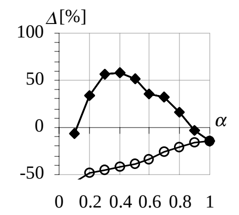

Figure 26. Δ
n.a. p=25% T_e=0.2

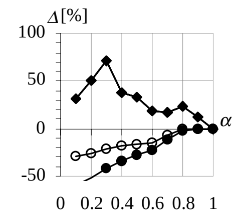

Figure 27. Δ
n.a. p=25% T_e=0.4

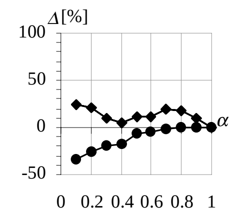

Figure 28. Δ
n.a. p=25% T_e=0.6

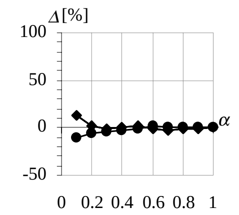

Figure 29. Δ
n.a. p=25% T_e=1.0

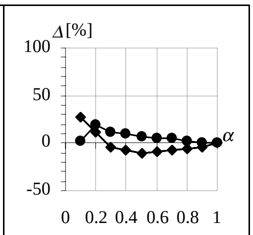

Figure 30. Δ
n.a. p=25% T_e=1.5

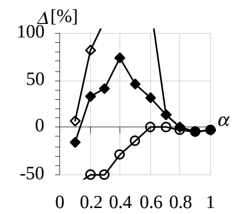

Figure 31. Δ
a.a. p=5% T_e=0.2

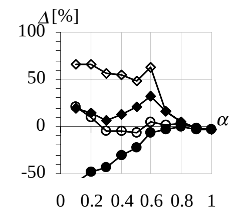

Figure 32. Δ
a.a. p=5% T_e=0.4

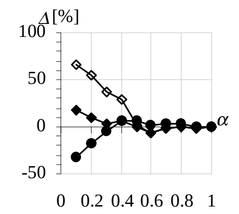

Figure 33. Δ
a.a. p=5% T_e=0.6

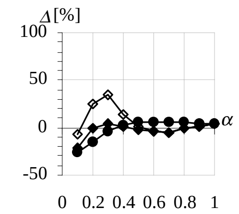

Figure 34. Δ
a.a. p=5% T_e=1.0

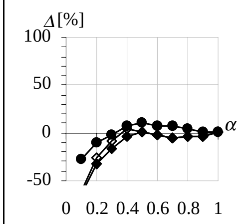

Figure 35. Δ
a.a. p=5% T_e=1.5

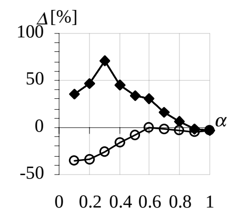

Figure 36. Δ
a.a. p=25% T_e=0.2

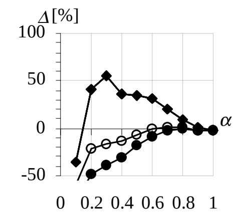

Figure 37. Δ
a.a. p=25% T_e=0.4

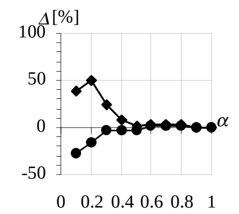

Figure 38. Δ
a.a. p=25% T_e=0.6

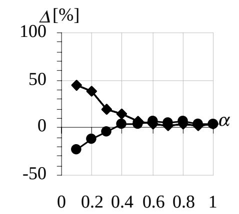

Figure 39. Δ
a.a. p=25% T_e=1.0

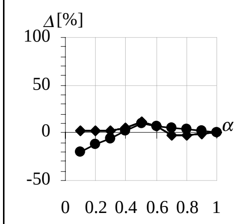

Figure 40. Δ
a.a. p=25% T_e=1.5

$VDRS_{NL}$ $VDRS_{12}$ EE ED

Further, for each model, in tables 2 - 5 the statistics of Δ(accelerogram type; p; T_e; α; *model*) (mean value μ_Δ, standard deviation σ_Δ, maximum Δ_{max} and minimum Δ_{min} value of the difference) are presented averaged over all T_e and α, for the two different values of p (5% and 25%).

	p = 5%				p = 25%			
Model	μ_Δ	σ_Δ	Δ_{max}	Δ_{min}	μ_Δ	σ_Δ	Δ_{max}	Δ_{min}
$VDRS_{NL}$	-15	19	52	-40	-13	10	14	-30
$VDRS_{12}$	45	90	387	-27	7	23	69	-26
ED - EE	3	17	45	-46	4	13	38	-36

Table 2. Statistics on Δ in percentage points for the elasto-yielding model and natural accelerograms

	p = 5%				p = 25%			
Model	μ_Δ	σ_Δ	Δ_{max}	Δ_{min}	μ_Δ	σ_Δ	Δ_{max}	Δ_{min}
$VDRS_{NL}$	-15	28	108	-61	-8	15	40	-24
$VDRS_{12}$	44	97	381	-52	12	28	83	-20
ED - EE	-2	10	12	-48	8	11	25	-35

Table 3. Statistics on Δ in percentage points for the elasto-yielding model and artificial accelerograms

	p = 5%				p = 25%			
Modello	μ_Δ	σ_Δ	Δ_{max}	Δ_{min}	μ_Δ	σ_Δ	Δ_{max}	Δ_{min}
$VDRS_{NL}$	2	21	80	-29	14	20	72	-15
$VDRS_{12}$	23	49	200	-18	14	20	72	-15
ED - EE	-10	19	15	-62	-11	17	19	-58

Table 4. Statistics on Δ in percentage points for the Takeda degrading model and natural accelerograms

	p = 5%				p = 25%			
Modello	μ_Δ	σ_Δ	Δ_{max}	Δ_{min}	μ_Δ	σ_Δ	Δ_{max}	Δ_{min}
$VDRS_{NL}$	4	20	74	-64	15	20	71	-35
$VDRS_{12}$	26	54	230	-62	15	20	71	-35
ED - EE	-5	16	21	-62	-6	13	10	-60

Table 5. Statistics on Δ in percentage points for the Takeda degrading model and artificial accelerograms

Let us examine the tables first. EE-ED yields globally the best approximation, followed by $VDRS_{NL}$ and $VDRS_{12.}$ In fact all its statistics are lower compared to the other two models. Figures 1 - 40 confirm the results shown in the tables. Errors increase for lower values of T_e, α and p. Essentially *VDRS* tend to over-estimate the displacements while *EE-ED* to under-estimate. This tendency of the *EE-ED* become more evident changing from artificial to natural accelerograms and from the elasto-yielding to the Takeda degrading model.

EXAMPLE APPLICATIONS

Two example applications of the whole procedure have been performed and are here illustrated. Both structures are existing and belong to the SS. Filippo e Nicola hospital in Avezzano, Italy, an area with a high seismic risk.

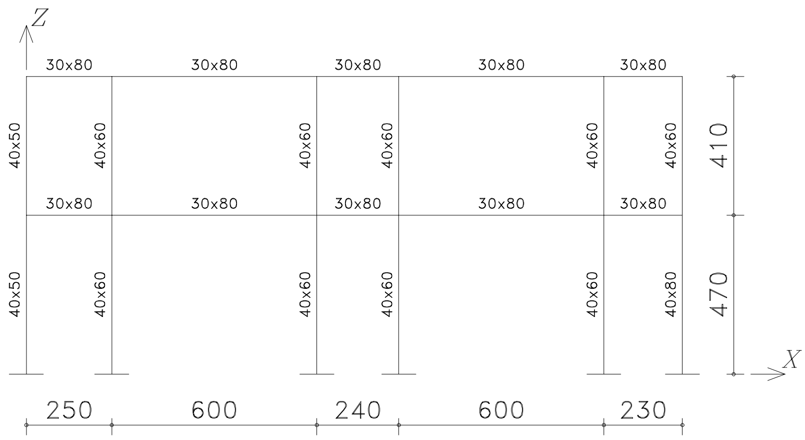

Figure 42. building A

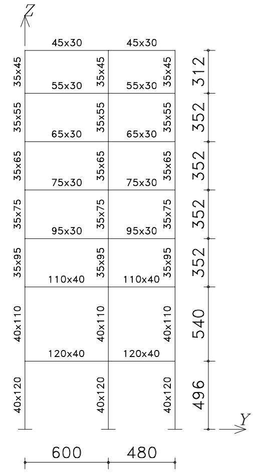

Figure 43. building B

The first structure, building A, is the two storey r.c. frame shown in fig. 42 (dimensions are in cm). Its elastic period T_e is of 0.335 sec and it is considered a good example for low period structures. The second building (B) is the seven storey r.c. frame shown in fig. 43, with T_e=1.596 sec and it is considered an example for high period structures. Modal and Push-over analysis on the buildings have given the capacity curve shown in figs. 44 and 45 and the values of table 6 for the parameters necessary to the VDRS's procedures

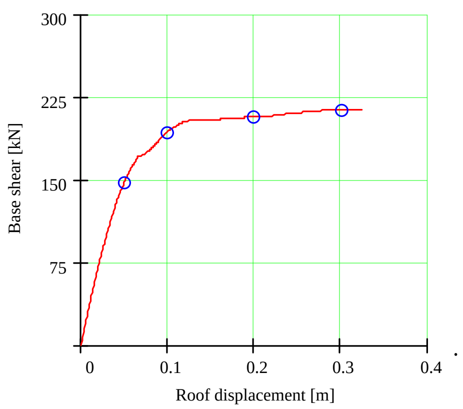

Figure 44. building A - capacity curve

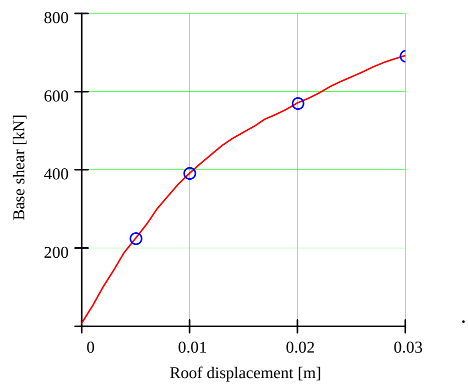

Figure 45. building B - capacity curve

building	PF_1	α_1	T_e [s]	a_y [ms^{-2}]	p [%]
A	1.212	0.925	0.335	1.435	5
B	1.381	0.764	1.596	0.459	27

Table 6. Parameters for VDRS's procedures

The curves were halted when the 2% interstorey drift was exceeded, following the recommendations in [ATC, 1996].

Displacements for the structures, under an earthquake EC8, soil B type, compatible, with p.g.a. = 1.0, 1.5, 2.0 ms^{-2} were computed with:

1. VDRS$_{NL}$, linearly interpolating between the PP of the cases p=5% and p=25% for both the elasto-yielding and Takeda degrading model

2. VDRS$_{12}$, linearly interpolating between the PP of the cases p=5% and p=25% for both the elasto-yielding and Takeda degrading model

3. EE-ED

4. The nine EC8 spectrum compatible accelerograms used before

The results of the study are in figs. 46 - 47 for buildings A and B, where continuous lines without symbols indicate the mean and the mean ± 1 standard deviation of the displacements computed with 4, continuous (dotted) lines with square symbols indicate those computed with 1 and 2 with elasto-yielding model - VDRS$_{12}$ is always above VDRS$_{NL}$ (Takeda degrading model - VDRS$_{12}$=VDRS$_{NL}$), continuous lines with circle symbols those computed with EE-ED (EE for building A, ED for building B).

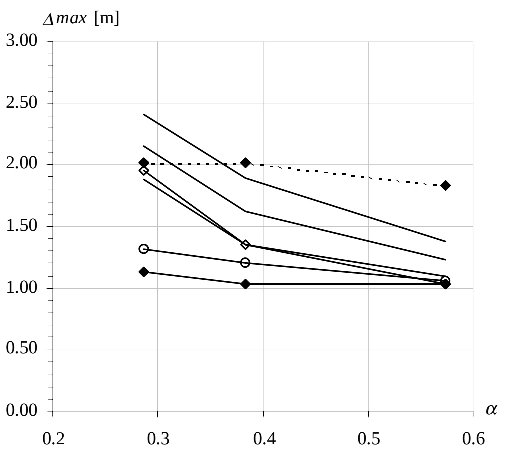

Figure 46. building A

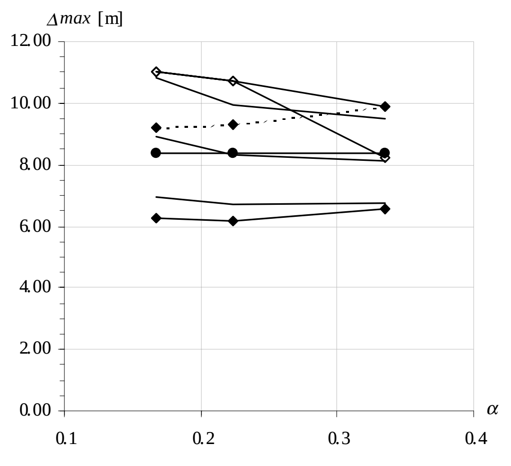

Figure 47. building B

VDRS NL-12 elasto-yielding | VDRS NL-12 Takeda | EE-ED | Numerical simulations

The error Δ as a function of α and fixed values of p and T_e is shown in figures 48 and 49.

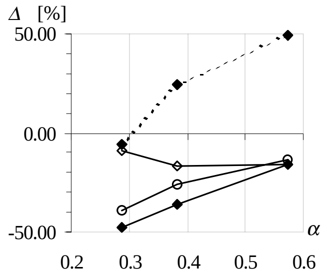

Figure 48. building A

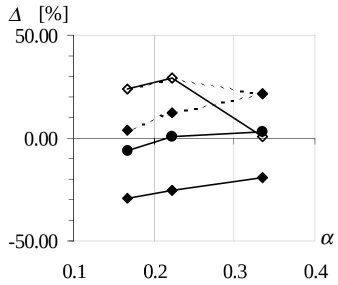

Figure 49. building B

For building A, $VDRS_{12.}$ yields globally the best approximation but under-estimate the displacements; only *VDRS* with Takeda degrading model tends to over-estimate the displacements. For building B, ED yields globally the best approximation, followed by VDRS with Takeda degrading model which tends to over-estimate the displacements.

CONCLUSIONS

The set of numerical tests performed to assess the accuracy of the ATC procedure – and thus of the simplifed VDRS one – indicate that it is relatively accurate, though, for elasto-plastic structures, traditional methods like the equal displacement or energy assumptions can be as accurate. The set of tests performed has been rather comprehensive, including two constitutive relationships for the sdof inelastic system (elasto – yielding and Takeda models) and tests on real structures. However since the ATC procedure permits to take into account also complex structural behavior, more representative of real structural response, finer setting of the procedure might succeed in improving its accuracy.

REFERENCES

Albanesi, T., Nuti, C., Vanzi, I (1999a): Seismic response of non linear structures using the concept of variable damping response spectrum, ISEE99, Montenegro

Albanesi, T., Nuti, C., Vanzi, I (1999b).: Risposta sismica di strutture non lineari usando il concetto di spettro di risposta a smorzameno variabile, convegno ANIDIS 99, Torino

ATC 40 (1996), “Seismic evaluation and retrofit of concrete buildings,” Report n. SSC 96-01

Chopra, A.K (1995)., “Dynamics of structures – Theory and Applications to Earthquake Engineering,” Prentice Hall, Inc., Englewood Cliffs, New Jersey

Eurocode 8 (1994), “Design provisions for earthquake resistance of structures,” ENV 1998, 1-1/-3, CEN, Brussels

Gulkan, *P*. and Sozen, M.A (1977)., “Inelastic responses of reinforced concrete structures to earthquake motions,” *Reinforced Concrete Structures in Seismic Zones*, N.M. Hawkins, Ed., ACI Publication SP-53, American Concrete Institute, Detroit, pp. 109-116

Miranda, E (1993), “Evaluation of site-dependent inelastic seismic design spectra,” *J. Struct. Engng.*, ASCE, 119(5), pp. 1319-1338

Paulay, T. and Priestley, M.J.N (1992)., “Seismic design of reinforced concrete and masonry buildings,” John Wiley & Sons, Inc., New York

Priestley, M.J.N (1997)., “Displacement-based seismic assessment of reinforced concrete buildings,” *Earthq. Engng. and Struct. Dyn.*, ICPress, Vol. 1, n. 1, , pp. 157-192.

P. Tsopelas, M.C. Constantinou, C.A. Kircher and A.S. Whittaker (1997), “Evaluation of simplified methods of analysis for yielding structures,” Report n. NCEER-97-0012